

ChemComm

Accepted Manuscript



This is an *Accepted Manuscript*, which has been through the Royal Society of Chemistry peer review process and has been accepted for publication.

Accepted Manuscripts are published online shortly after acceptance, before technical editing, formatting and proof reading. Using this free service, authors can make their results available to the community, in citable form, before we publish the edited article. We will replace this *Accepted Manuscript* with the edited and formatted *Advance Article* as soon as it is available.

You can find more information about *Accepted Manuscripts* in the [Information for Authors](#).

Please note that technical editing may introduce minor changes to the text and/or graphics, which may alter content. The journal's standard [Terms & Conditions](#) and the [Ethical guidelines](#) still apply. In no event shall the Royal Society of Chemistry be held responsible for any errors or omissions in this *Accepted Manuscript* or any consequences arising from the use of any information it contains.

COMMUNICATION

Activation of carbon-supported catalysts by ozonized acidic solutions for the direct implementation in (electro-)chemical reactors

Cite this: DOI: 10.1039/x0xx00000x

Received 00th January 2012,

Accepted 00th January 2012

DOI: 10.1039/x0xx00000x

www.rsc.org/

C. Baldizzone^a, S. Mezzavilla^b, N. Hodnik^a, A. R. Zeradjanin^a, A. Kostka^c, F. Schüth^b and K.J.J. Mayrhofer^a

This work introduces a practical and scalable post-synthesis treatment for carbon-supported catalysts designed to achieve complete activation and, if necessary, simultaneously surface dealloying. The core-concept behind the method is to control the potential without utilizing any electrochemical equipment, but rather by applying an appropriate gas mixture to a catalyst suspension.

In the past years fuel cells have received substantial attention from the scientific community, as they represent a promising technology for energy conversion¹. However, for this technology to reach the high reliability standards required by large scale application still several issues need to be solved². Above all, the development of a scalable synthesis of a highly active and stable catalyst is pivotal. The scientific literature offers a plethora of materials, ranging from Pt-based to platinum-free catalyst assemblies²⁻³, with platinum based catalyst still being the most realistic solution^{2,4}. Nanoscale Pt alloys can be obtained by numerous approaches⁵. Yet, a common issue to most of the synthesis routes is the preparation of chemically homogeneous catalysts readily implementable in a fuel cell^{5b,6}. In reality, in the early life stages of a catalyst (also labelled “as-synthesized”) the active surfaces are often blocked by impurities and/or carbonaceous residues left by the synthesis process, which can seriously hinder the desired reactions^{5b,7}. Even though heterogeneous catalysis offers a few solutions, e.g. oxidative purification by acid solution and/or annealing at high temperature⁸, such processes are not easily transferrable to electrocatalysis. Currently such pollutants are usually removed by mild annealing, by post-synthesis oxidation and in fundamental studies by at least few electrochemical potential excursions to high potentials; even for pure Pt catalysts^{6,9}. Moreover, by introducing alloying elements homogeneously dispersed in the Pt framework the need of an activation protocol becomes even more compelling, as the non-noble element needs to be removed from the surface layers¹⁰. For this purpose several techniques are available^{9,11}, namely chemical and electrochemical dealloying. However, while the former is often unable to produce stable core-shell structures^{10,12} and does not remove undesired residual carbon, the latter cannot be implemented within a fuel cell stack and is typically not applicable as a large scale post-synthesis process^{3c,13}. An exemplary material class where these issues of activation become especially important, are the promising

alloy nanocatalysts on mesostructured supports, as for instance in the shape of hollow graphitic spheres (PtTM @ HGS). A detailed description of the preparation of such HGS and of the nanoparticles is reported in the Supplementary Information and in our previous work^{7a,14}.

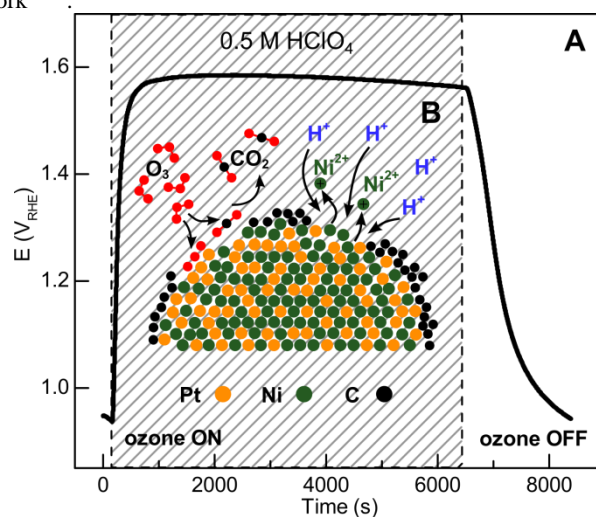


Fig. 1: Time evolution of the open circuit potential in presence of ozone (A) and schematic representation of the activation/dealloying process proceeding at the catalyst surface (B). The measurement was carried out in a 0.5 M HClO₄ solution at room temperature during O₃ bubbling.

The physical separation of the nanoparticles within the mesoporous support, i.e. pore confinement effect, was found effective in ensuring an optimal particle size distribution, suppressing high temperature sintering during the synthesis process, and in preventing some of the degradation mechanisms relevant to fuel cell operation, e.g. agglomeration and detachment. However, during the annealing treatment at high temperature (850°C, 7h), a carbon layer grows on the active particles, which blocks the catalyst surface and thus the reaction on the as-prepared samples. The presence of such surface films was recently verified by our electrochemical analysis and corroborated by a detailed EXAFS study¹⁴. So far, the attempts to activate the catalyst ex-situ by acid-leaching in different acidic media, e.g. HClO₄ and HCl, and 2 hours annealing at 350°C in air

were not able to completely remove the protective NiC layer (Figure S3). These approaches have yielded in the best case a partially activated material, so that, up to now, to reach complete initial activation an intense cycling to highly positive potentials (i.e. 200 cycles up to $1.4V_{RHE}$, Figure S2) has been required. However, applying this procedure to remove the carbon layer and to selectively leach the less noble metal from the alloy close to the surface layers within a fuel cell stack is not advisable, as all the surface species and less noble elements removed from the catalyst may then redeposit on other components of the system, leading to poisoning and loss in performance¹³.

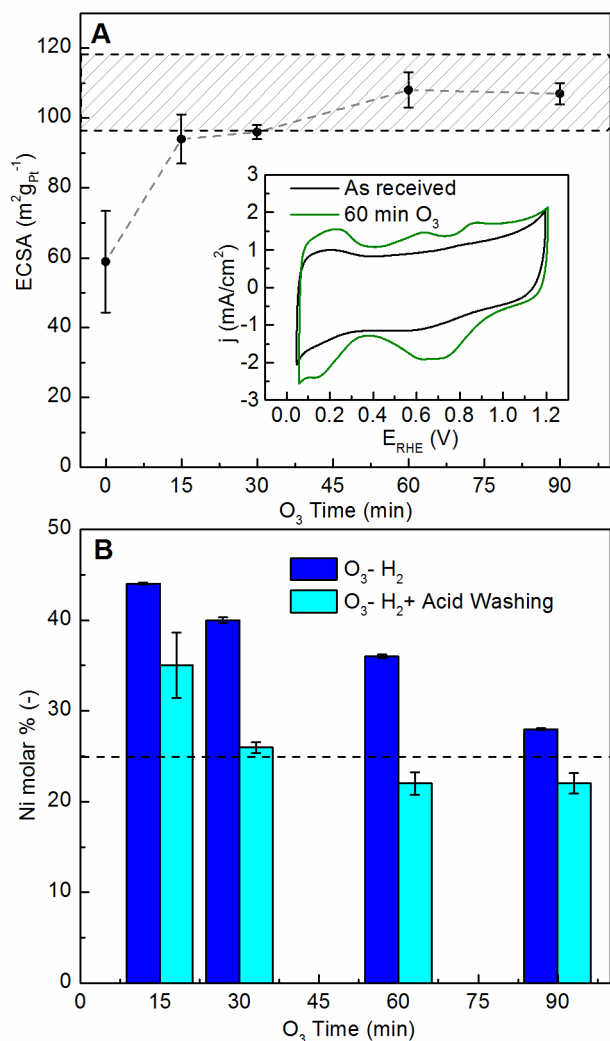


Fig.2: (A) Evolution of ECSA measured by CO-stripping versus ozone treatment time and representative CVs between 0.05 and 1.2 V_{RHE} with 0.05 V/s scan rate of the catalyst before and after O₃ activation (inset). The gray shaded area indicates the ECSA range expected for PtNi@HGS activated by electrochemical cycling, whereas zero time in O₃ corresponds to the as-received samples after synthesis. (B) Progress of dealloying, i.e. decrease of Ni molar ratio, measured by ICP-MS versus time in ozone, the dashed black line corresponds to the Ni content after electrochemical dealloying.

In order to circumvent the issues of in-situ activation and to develop a procedure for the preparation of alloy nanocatalysts to be used as synthesized, we have utilized ozone treatment as a new scalable mean. Ozone is a reactant that is known for its high oxidizing power¹⁵. There are a few examples concerning the use of ozone in heterogeneous catalysis, mainly focused on coke-removal¹⁶ and purification/functionalization of carbon materials, e.g. CNTs and

graphene¹⁷. Moreover, Kucernak et al.^{15c} offer a nice example on how purging ozone in a fuel cell stack could efficiently remove pollutants adsorbed on the Pt surfaces. In this study we utilize ozone gas purged into an acidic solution for a facile post synthesis process, in order to achieve simultaneously the removal of synthesis by-products and the formation of a fully developed dealloyed structure for platinum based nanocatalyst. Before applying the ex-situ treatment, we confirmed the effect of ozone in an electrochemical experiment (see Fig. 1). When ozone is purged into an acidic solution, the open circuit potential (OCP) of a Pt-based catalyst rapidly increases to around 1.6 V_{RHE} . The natural equilibrium on the surface between oxygen reduction and surface oxidation shifts to an equilibrium between ozone reduction and oxygen/peroxide oxidation. Thus, ozone purging can, via purely chemical means, in general mimic the effect of excursions to positive potentials in an electrochemical experiment, rendering this approach applicable for large scale synthesis procedures of nanocatalysts. The experimental apparatus for an ex-situ ozone treatment is utterly simple and consists of bubbling a steady flow of O₃ inside a vessel containing the catalyst dispersed in a 0.5 M HClO₄ solution. The catalyst was then collected and dried to be reduced in a tubular furnace under a H₂ atmosphere (50 °C, 1.5 hours). Moreover, as the reductive step is carried out in gas phase, a further acid washing in 0.1 M HClO₄ is implemented to ensure total removal of any leftover surface nickel which might get exposed by the reduction of the Pt oxides¹⁸. In order to investigate the effectiveness of the ex-situ ozone approach, different treatment times are considered, i.e. 15, 30, 60 and 90 minutes. After the treatment, the materials were examined by means of Transmission Electron Microscopy (TEM) in order to verify whether the initial morphology is maintained. Figure S5 includes high-magnification images of the HGS at different times proving that both the hollow sphere configuration and the mesoporous nature of the support is maintained, regardless of the duration of the treatment. In the following, the work concentrates on a detailed characterization of the electrochemical performances of the catalyst by means of thin-film Rotating Disk Electrode technique (RDE). Figure 2 includes the effect of time in O₃ versus the crucial processes of Pt surface evolution (activation, Fig.2A), i.e. removal of carbon and of the surface alloying element (dealloying, Fig.2B). The extent of the activation is investigated by the electrochemical surface area (ECSA) measured by CO-stripping after certain treatments, whereas the dealloying is monitored by measuring the Ni molar ratio utilizing Inductively Couple Plasma Mass Spectrometer (ICP-MS). Once the ozone is introduced in the system the removal of the blocking species appears to proceed quite rapidly, as already after 15 minutes the ECSA reaches the lower limit of the surface area range expected for fully activated PtNi@HGS, i.e. the gray shaded area. Extending the duration of the ozone treatment, the ECSA becomes larger and complete activation is reached after 60 minutes, as supported by the fully developed Pt features displayed in the inset of Figure 2A. An effect of O₃ on the size of the nanoparticles and in turn on the ECSA is excluded by the Particle Size Distribution (PSD) analysis for all the different treatment times (Figure S5). As reported in the SI, both average diameter and PSDs are similar, regardless of the length of ozone exposure, indicating the removal of blocking species as the sole reason for the observed increase in ECSA. Given the high oxidizing power of ozone and the presence of an acidic media, the carbon removal can proceed by a chemical and/or an electrochemical route. The former includes direct reaction of the carbon with the ozone and the indirect reaction through radical intermediates^{15a, 15b}, while the latter consists of carbon oxidation triggered by the high potential related to the ozone reduction (Figure S1). Note that the ozone treatment initiates a parallel process to the catalyst activation, namely the formation of oxygen groups on the carbon support, as

supported by the progressively growing peak around 0.6 V_{RHE} (Figure S4). This peak is usually ascribed to the electroactive hydroquinone/quinone couple and its formation is usually considered an indication of carbon oxidation/corrosion. Although these species are the only detectable by electrochemical techniques, they only account for a minor fraction of the several possible oxygen groups generated by electrochemical oxidation and/or chemical reaction with ozone intermediates. However, the focus of this work is not investigating the nature of the surface chemistry modification of the support, but rather only assessing its eventual effect on the stability and activity of the material. Beside carbon corrosion, another possible reaction promoted by the high potential related to O_3 reduction is platinum dissolution¹⁹. Accordingly, the Pt loading after the O_3 - H_2 activation protocol has been analyzed and is displayed in Figure S7. For all samples no Pt loss can be detected within the uncertainty of the measurement, with the exception of the sample treated for 90 min for which a small decrease of around 7% is observed. On the other hand, the dealloying process appears to proceed at slower rates compared to the carbon removal, with an almost linear decrease of the Ni molar ratio with O_3 time (Figure 2B). However, by implementing a further acid washing the nickel removal is brought to a larger extent and the Ni molar ratio after 60 minutes reaches a plateau of around 22%, a value slightly below the expected 25 at.% Ni content for electrochemically dealloyed PtNi@HGS (black dashed line in Figure 2B). A possible explanation is that nickel dissolution occurs in two separate instances, during the ozone step, by direct oxidation, and after the reductive step. Indeed, the reduction of the Pt oxide induces the formation of a rougher surface, exposing the nickel in the inner layers of the nanoparticle¹⁸. The consequences of the ozone treatment were additionally followed by means of XRD (Figure S8). Upon increasing treatment time, the reflection intensity associated to the alloy (PtNi) phase progressively decreases and, concurrently, a broad shoulder between 30–45° 2 θ becomes more pronounced. This evolution can be ascribed to the formation of a progressively thicker (though poorly crystalline) Pt oxide layer on the PtNi NPs surface which, inherently, causes the parallel reduction in degree of crystallinity of the metallic alloy phase. A simple gas-phase treatment (50°C, 1.5 h) in H_2/Ar (15%) is sufficient to reduce the Pt-O layer (Figure S8). After this step, the shoulder associated to the oxide phase has completely vanished and, simultaneously, the intensity of the reflections corresponding to the metallic phase is partially restored. Here it is to note that after this two-step treatment the PtNi pattern is shifted towards lower angle compared to the position measured with the initial (as-received) catalyst. This lattice expansion, consequence of the removal of Ni atoms from the alloy NPs, is especially visible for the sample treated in O_3 for 90 min, whereas it is barely appreciable for the sample treated only for 15 min (Figure S9). Such findings are in agreement with the residual Ni content evaluated via ICP-MS and confirm the O_3 effectiveness for dealloying (when a sufficient long treatment is applied). Once complete activation/dealloying is achieved, the electrochemical properties of the O_3 -activated samples are compared with the catalyst activated by conventional electrochemical cycling (EC activated), assessing whether ozone has a detrimental effect on the catalytic performances, namely stability (Figure 3A) and activity (Figure 3B). Stability is evaluated by cycling the catalyst for 10800 cycles between 0.4 and 1.0 V_{RHE} , a common potential window for ORR in fuel cell operation, and monitoring the active surface area by CO-stripping, Figure 2A shows the ECSA evolution for every O_3 pre-treatment time considered. The samples treated for 15 and 30 minutes show a slight increase in ECSA during the degradation protocol, which is reasonable considering an incomplete activation process. In contrast, 90 minutes treatment yields a small drop in active surface area of around 10% (Figure 3A, inset). It is likely that

prolonged exposure to the highly oxidizing conditions of O_3 could have an effect on both the carbon support and the platinum dissolution behavior. On one hand, carbon corrosion triggered by the ozone reduction could partially disintegrate the mesoporous network of the spheres, weakening the pore confinement of the nanoparticles, while on the other hand a too thick Pt oxide layer due to extended time at high potential could lead to enhanced dissolution. In spite of that, exposing the catalyst to O_3 for 60 minutes appears to provide a perfect intermediate condition, showing complete activation from the beginning of the degradation protocol and negligible ECSA losses during cycling.

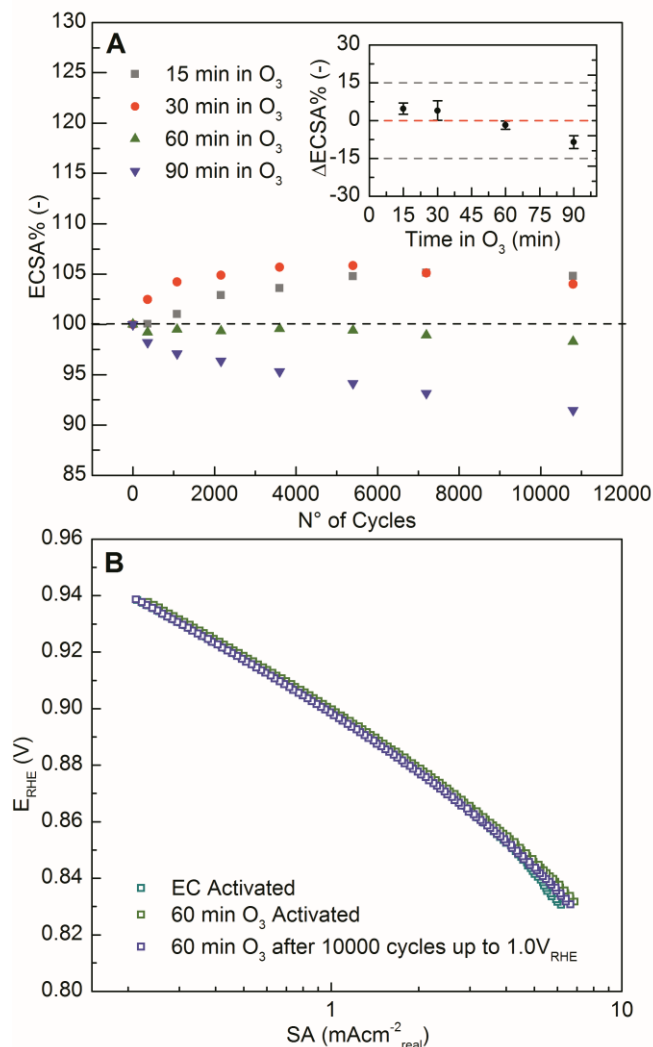


Fig.3: (A) Evolution of normalized ECSA with cycles and ΔECSA before and after 10800 cycles between 0.4 and 1.0 V_{RHE} at 1.0 V/s scan rate (inset). (B) Intrinsic activity comparison by means of Tafel plots of the PtNi@HGS electrochemically activated (EC), O_3 activated before and after 10000 cycles between 0.4 and 1.0 V_{RHE} at 1.0 V/s scan rate.

The specific activity (SA) of the O_3 activated catalyst for 60 minutes, which was found the most suitable process time, appears to completely match the performance of the EC activated counterpart (Figure 3B). Obviously ozone is able to completely remove the NiC protective layer, producing a material fully accessible to the electrolyte and reactants like oxygen and unimpaired by material specific mass transport issues. Most important, no further cleaning cycles to high potentials are applied before the activity test, indicating that the material is activated from the first cycle. Moreover, as the nickel ratio and intrinsic activity are similar for

both O₃ and EC activated catalyst, it is reasonable to identify the alloying element content as the sole parameter affecting the ORR specific activity. Indeed, the modifications of the carbon support during the ozone pre-treatment appear not to have any influence on the catalytic performance of the material. Finally and most important, the stability against further dissolution of the alloying element was investigated. In this regard, Figure 3B displays the Tafel plots of the 60 minutes O₃ activated PtNi@HGS before and after a degradation protocol of 10000 cycles between 0.4 and 1.0 V_{RHE}, showing a complete retention of the specific activity and proving that the dealloyed surface layers developed during activation are fully capable to prevent further leaching of nickel during the ORR. In conclusion, an ozonized acidic solution was successfully employed to reach complete activation and simultaneous surface dealloying of the catalyst under study. Where conventional ex-situ methods like acid washing failed, the ozone method was able to provide fully accessible and stable dealloyed structures ready to be utilized directly after synthesis. The catalytic properties of the ozone treated samples are comparable to the material activated by in-situ high potential cycling, proving that employing O₃ and H₂ effectively mimic the effect of electrochemical activation with no detrimental consequence on the catalyst performance. Albeit the current work deals with a specific type of electrocatalyst material, the ozone approach represents a promising technique easily transferrable to other classes of (Pt based-) catalysts prepared via different synthesis routes, i.e. solvothermal colloidal methods. This approach is particularly useful in activation of larger quantities of (electro-) catalysts, where activation “by electrode” would be highly difficult if not impossible.

Thanks are given to A. Mingers for the assistance with the ICP-MS measurements. Moreover, C.B acknowledges the IMPRS-SurMat for funding. Also funding by the DFG in the framework of the AIF/DFG fuel cell cluster is gratefully acknowledged.

Notes and references

^a Dept. of Interface Chemistry and Surface Engineering, Max Planck Institut für Eisenforschung GmbH, Max-Planck-Strasse 1, 40237 Düsseldorf, Germany

^b Dept. of Heterogeneous Catalysis, Max Planck Institut für Kohlenforschung, Kaiser-Wilhelm-Platz 1, 45470 Mülheim an der Ruhr, Germany

^c Dept. of High Temperature Materials, Max Planck Institut für Eisenforschung GmbH, Max-Planck-Str. 1, 40237 Düsseldorf, Germany

- aI. Katsounaros, S. Cherevko, A. R. Zeradjanin and K. J. J. Mayrhofer, *Angewandte Chemie International Edition*, 2014, **53**, 102-121; bH. A. Gasteiger and N. M. Marković, *Science*, 2009, **324**, 48-49.
- M. K. Debe, *Nature*, 2012, **486**, 43-51.
- aT. Toda, H. Igarashi, H. Uchida and M. Watanabe, *Journal of The Electrochemical Society*, 1999, **146**, 3750-3756; bA. Rabis, P. Rodriguez and T. J. Schmidt, *ACS Catalysis*, 2012, **2**, 864-890; cH. A. Gasteiger, S. S. Kocha, B. Sompalli and F. T. Wagner, *Applied Catalysis B: Environmental*, 2005, **56**, 9-35.
- V. Goellner, C. Baldizzone, A. Schuppert, M. T. Sougrati, K. Mayrhofer and F. Jaouen, *Physical Chemistry Chemical Physics*, 2014, **16**, 18454-18462.
- aT. Ghosh, B. M. Leonard, Q. Zhou and F. J. DiSalvo, *Chemistry of Materials*, 2010, **22**, 2190-2202; bB. M. Leonard, Q. Zhou, D. Wu and F. J. DiSalvo, *Chemistry of Materials*, 2011, **23**, 1136-1146; cJ. Zhang, K. Sasaki, E. Sutter and R. R. Adzic, *Science*, 2007, **315**, 220-222; dT. S. Ahmadi, Z. L. Wang, T. C. Green, A. Henglein and M. A. El-Sayed, *Science*, 1996, **272**, 1924-1925; eD. Wang, L. Zhuang and J. Lu, *The Journal of Physical Chemistry C*, 2007, **111**, 16416-16422.
- D. Li, C. Wang, D. Tripkovic, S. Sun, N. M. Markovic and V. R. Stamenkovic, *ACS Catalysis*, 2012, **2**, 1358-1362.
- aC. Galeano, J. C. Meier, V. Peinecke, H. Bongard, I. Katsounaros, A. A. Topalov, A. Lu, K. J. J. Mayrhofer and F. Schüth, *Journal of the American Chemical Society*, 2012, **134**, 20457-20465; bD. Wang, H. L. Xin, Y. Yu, H. Wang, E. Rus, D. A. Muller and H. D. Abruña, *Journal of the American Chemical Society*, 2010, **132**, 17664-17666.
- aA. Rinaldi, J. Zhang, B. Frank, D. S. Su, S. B. Abd Hamid and R. Schlögl, *ChemSusChem*, 2010, **3**, 254-260; bA. Rinaldi, B. Frank, D. S. Su, S. B. A. Hamid and R. Schlögl, *Chemistry of Materials*, 2011, **23**, 926-928.
- D. Wang, H. L. Xin, R. Hovden, H. Wang, Y. Yu, D. A. Muller, F. J. DiSalvo and H. D. Abruña, *Nat Mater*, 2013, **12**, 81-87.
- M. Oezaslan, F. Hasché and P. Strasser, *The Journal of Physical Chemistry Letters*, 2013, **4**, 3273-3291.
- aF. Hasché, M. Oezaslan and P. Strasser, *ECS Transactions*, 2011, **41**, 1079-1088; bC. Wang, M. Chi, D. Li, D. Strmcnik, D. van der Vliet, G. Wang, V. Komanicky, K.-C. Chang, A. P. Paulikas, D. Tripkovic, J. Pearson, K. L. More, N. M. Markovic and V. R. Stamenkovic, *Journal of the American Chemical Society*, 2011, **133**, 14396-14403; cK. Sasaki, H. Naohara, Y. Cai, Y. M. Choi, P. Liu, M. B. Vukmirovic, J. X. Wang and R. R. Adzic, *Angewandte Chemie International Edition*, 2010, **49**, 8602-8607; dJ. Snyder, K. Livi and J. Erlebacher, *Advanced Functional Materials*, 2013, **23**, 5494-5501.
- J. Durst, M. Lopez-Haro, L. Dubau, M. Chatenet, Y. Soldo-Olivier, L. Guétaz, P. Bayle-Guillemaud and F. Maillard, *The Journal of Physical Chemistry Letters*, 2014, **5**, 434-439.
- J. Durst, M. Chatenet and F. Maillard, *Physical Chemistry Chemical Physics*, 2012, **14**, 13000-13009.
- C. Baldizzone, S. Mezzavilla, H.W.P.Carvalho, J.C. Meier, A.K. Schuppert, M. Heggen, C. Galeano, J-D. Grunwaldt, F. Schüth and K.J.J. Mayrhofer, *Angewandte Chemie International Edition*, 2014, DOI: 10.1002/anie.201406812R1.
- aK. Sehested, J. Holcman, E. Bjergbakke and E. J. Hart, *The Journal of Physical Chemistry*, 1987, **91**, 2359-2361; bK. Sehested, H. Corfitzen, J. Holcman and E. J. Hart, *The Journal of Physical Chemistry*, 1992, **96**, 1005-1009; cB. K. Kakati and A. R. J. Kucernak, *Journal of Power Sources*, 2014, **252**, 317-326.
- C. L. Pieck, C. R. Vera, C. A. Querini and J. M. Parera, *Applied Catalysis A: General*, 2005, **278**, 173-180.
- aW. Gao, G. Wu, M. T. Janicke, D. A. Cullen, R. Mukundan, J. K. Baldwin, E. L. Brosha, C. Galande, P. M. Ajayan, K. L. More, A. M. Dattelbaum and P. Zelenay, *Angewandte Chemie International Edition*, 2014, **53**, 3588-3593; bH. Valdés, M. Sánchez-Polo, J. Rivera-Utrilla and C. A. Zaror, *Langmuir*, 2002, **18**, 2111-2116.
- A. K. Schuppert, A. Savan, A. Ludwig and K. J. J. Mayrhofer, *Electrochimica Acta*, 2014, **144**, 332-340.
- aA. A. Topalov, S. Cherevko, A. R. Zeradjanin, J. C. Meier, I. Katsounaros and K. J. J. Mayrhofer, *Chemical Science*, 2014, **5**, 631-638; bA. A. Topalov, I. Katsounaros, M. Auinger, S. Cherevko, J. C. Meier, S. O. Klemm and K. J. J. Mayrhofer, *Angewandte Chemie International Edition*, 2012, **51**, 12613-12615.